Measurements of Inclusive and Exclusive Diffraction at HERA *

Armen Bunyatyan[a]

[a] Max-Planck-Institut für Kernphysik,
Saupfercheckweg 1, 69117 Heidelberg, Germany
and Yerevan Physics Institute, Armenia
E-mail: bunar@mail.desy.de

Representing the H1 and ZEUS Collaborations

Recent measurements of inclusive processes, vector meson production and hadronic final states in diffractive interactions at HERA are presented. The data is used to investigate the factorization properties and study the partonic structure of colour singlet exchange. Resolved Pomeron and colour dipole models are compared with the data.

1. Introduction

In the first running period, which ended in 2000, the ep collider HERA delivered more than $100pb^{-1}$ of integrated luminosity for each of the two experiments H1 and ZEUS. This data allows many interesting physics topics to be studied with high precision. In this report we present some recent results on diffractive physics.

The diffractive dissociation of the photon $\gamma p \to Xp$ has characteristics similar to diffractive hadron–hadron interactions and can be described by Regge phenomenology. Within this framework, diffractive interactions at high energies are dominated by the exchange of the Pomeron, an object with vacuum quantum numbers. One of the predictions of this approach is a slow rise of the cross section with the center-of-mass energy W, i.e. $\sigma \propto W^{0.2-0.3}$ [1].

On the other hand, perturbative QCD (pQCD) calculations can be made for diffractive processes in which a hard scale is present: processes with high virtuality Q^2 or high four-momentum transfer squared $|t|$, jets and charm production. In pQCD the vacuum exchange can be modelled as a exchange of a colour singlet gluon ladder between the proton and the virtual photon which fluctuates into a $q\bar{q}$ or $q\bar{q}g$ state before the interaction. In this approach, the cross section is factorized into the square of the effective dipole wave function and the square of the cross section for diffractive scattering of the dipole off the pro-

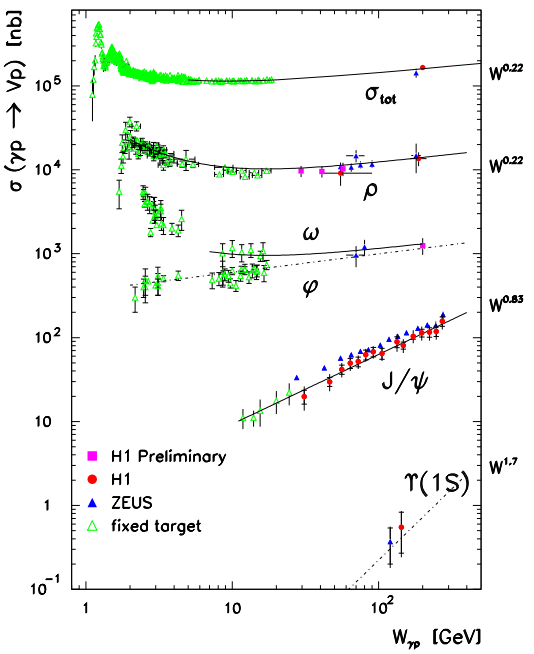

Figure 1. Vector meson cross sections as a function of the total CM energy of the photon-proton system $W_{\gamma p}$ in photoproduction ($Q^2 = 0$).

*Talk given at the International Conference QCD 02, July 2–9, Montpellier, France

ton [2]. There are several "colour dipole" models which differ in the way they treat the dipole-proton interaction.

At HERA, it is possible to vary the scale with which the Pomeron structure is probed in diffractive interactions, to study its partonic content and the transition from soft to hard interactions.

2. Diffractive Vector Meson Production

Vector meson production has been extensively studied at HERA both in the photoproduction ($Q^2 \sim 0$) and DIS regimes ($Q^2 > 1\ GeV^2$). Figure 1 presents the exclusive photoproduction cross section for different vector mesons as a function of the γp center of mass energy, $W_{\gamma p}$ [3,4]. The cross sections for light vector mesons (ρ, ω, ϕ) follow the soft behaviour of the total photon–proton cross section parameterized as $\sim W^{0.2}$ in agreement with the predictions of the Regge approach [1]. In contrast, the J/ψ cross section exhibits much harder energy dependence ($\sim W^{0.8}$) [5,6]. Here, the mass of the charm quark sets the hard scale for pQCD calculations, and the steep energy dependence, which is related to the rise of the gluon density in the proton at small values of Bjorken-x, is quite well described by pQCD predictions [7,8] (see Figure 2). More data will allow discrimination between the different theoretical models.

Figure 3 shows the ρ cross section for different values of Q^2 as a function of W [9]. The energy dependence of the cross section becomes steeper as Q^2 increases. For light vector mesons, Q^2 plays the role of the hard scale, similar to the mass of the charm quark in the case of J/ψ photoproduction.

3. Inclusive Diffraction in DIS

The kinematics of diffractive deep inelastic scattering, $ep \rightarrow eXp$ (Figure 4), can be expressed in terms of the photon virtuality Q^2, the squared four momentum transfer t, Bjorken x, the fraction of the beam protons momentum carried by the Pomeron, $x_{I\!P}$, and the fraction of the Pomeron's momentum carried by struck quark, β.

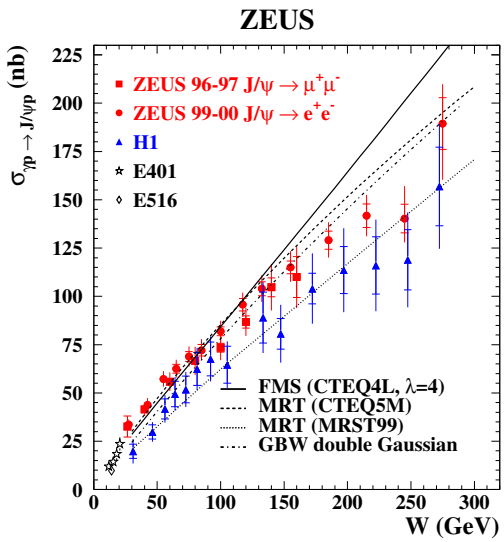

Figure 2. The J/ψ meson cross section as a function of $W_{\gamma p}$ in photoproduction ($Q^2 = 0$) compared with pQCD calculations.

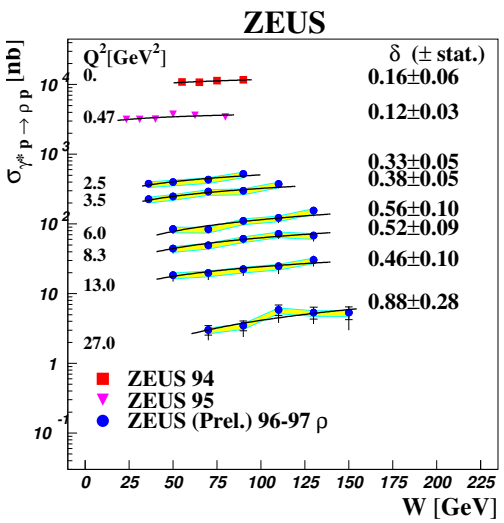

Figure 3. The ρ meson cross section as function of $W_{\gamma p}$ at different values of Q^2.

The cross section for the diffractive DIS process can be described by an expression analogous to that used for inclusive DIS:

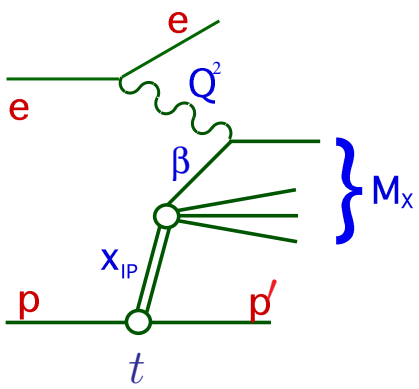

Figure 4. A diagram of diffractive ep interactions and the definition of the various kinematic variables used to describe diffractive process.

$$\frac{d\sigma^D}{d\beta dQ^2 dx_{I\!P}} = \frac{2\pi\alpha}{\beta Q^4}(1-y+y^2/2)\cdot\sigma_R^{D(3)}(\beta, Q^2, x_{I\!P}),$$

where $\sigma_R^D = F_2^D - \frac{y^2}{1+(1-y)^2}F_L^D$ is the "reduced diffractive cross section" which is equal to the diffractive structure function F_2^D if it is assumed that $F_L^D = 0$.

In Figures 5 and 6, the new high precision H1 measurements of $\sigma_R^{D(3)}(\beta, Q^2, x_{I\!P})$ are shown as a function of Q^2 and β for different $x_{I\!P}$ bins [10]. From these distributions the following properties of diffractive structure functions are deduced:

- relatively flat β dependence,
- strong scaling violation rising with $ln(Q^2)$ up to relatively large β.

There is an obvious difference between the Q^2 and x (or β) dependences of the diffractive structure function F_2^D and the proton structure function F_2 which can be related to the very large gluon component in the diffractive case.

These measurements are subjected to a DGLAP QCD analysis in order to extract diffractive parton densities which, for example, can be used in Monte Carlo programs to make predictions for hadronic final states in diffractive processes. This analysis also allows the testing of QCD hard scattering factorization theorem for semi-inclusive DIS [11]. According to this theorem, the diffractive structure function can be factorized into the product of the pQCD hard scattering cross section $\hat{\sigma}(x, Q^2)$ and the diffractive parton density functions (PDFs) $f^D(x_{I\!P}, t, x, Q^2)$. The PDFs obey the DGLAP evolution equations and are universal for diffractive DIS processes. In addition, Regge factorization between the $(x_{I\!P}, t)$ and (x, Q^2) dependences is assumed, according to which the Pomeron PDF is independent of $x_{I\!P}$ and t.

The extracted NLO singlet-quark $\Sigma(z, Q^2)$ and gluon densities $g(z, Q^2)$, together with their uncertainties, are shown in Figure 7 [12]. Here the variable z corresponds to the momentum fraction carried by an individual parton. The QCD fit describes the β and Q^2 evolution very well (Figures 5 and 6). The comparison of quark and gluon contributions shows that up to 75% of the Pomeron momentum is carried by gluons. It is also apparent that due to the indirect extraction

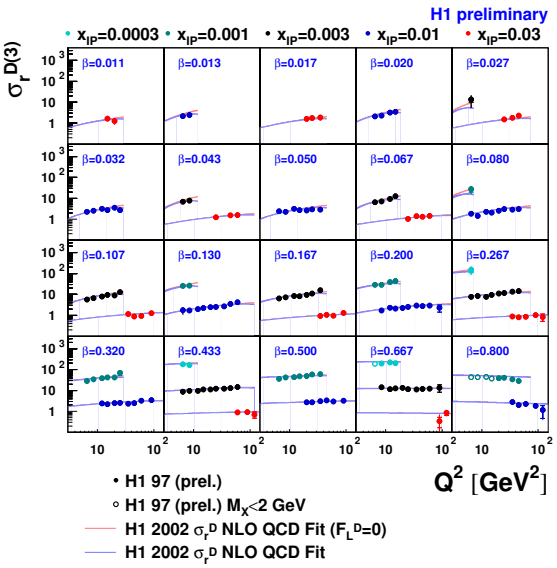

Figure 5. Q^2 dependence of the reduced cross section at fixed $x_{I\!P}$ and fixed β compared with the predictions of the NLO QCD fits.

of $g(z, Q^2)$ from the scaling violation, the gluon densities at high z have large uncertainties.

4. Diffractive Dijet and Charm Production

According to the QCD factorization theorem, the parton distribution functions extracted from the QCD fits to diffractive structure functions can be used to describe hadronic final states in diffractive DIS. Of particular interest are measurements of open charm, $\gamma^* q \to c\bar{c}$ and diffractive dijet production since the boson–gluon fusion process provides a direct probe of the gluon content of the Pomeron, in contrast to inclusive measurements. The presence of a hard scale provided by the high transverse momentum of the jets or the mass of the charm quark allows the testing of different QCD based models.

The PDFs extracted from the LO QCD fits have been implemented in the RAPGAP Monte Carlo generator [13] and used to make predictions for various hadronic final state observables. Figure 8 shows the cross section for diffractive dijet

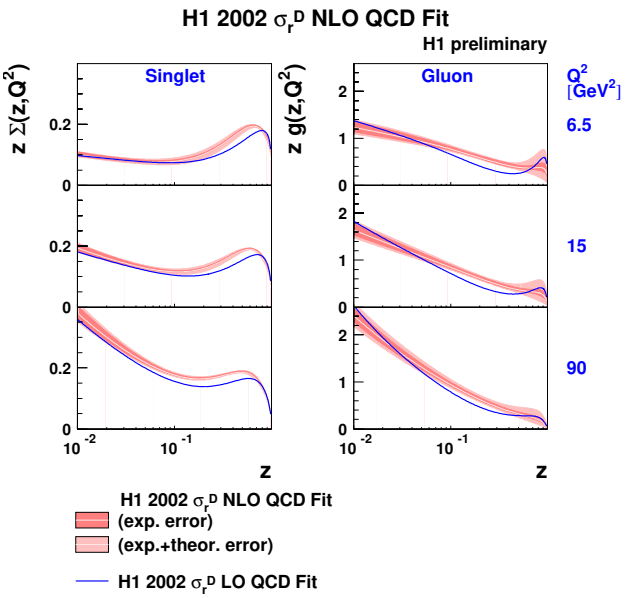

Figure 7. Pomeron parton densities. The left hand side shows the singlet quark distribution, the right hand side shows the gluon density.

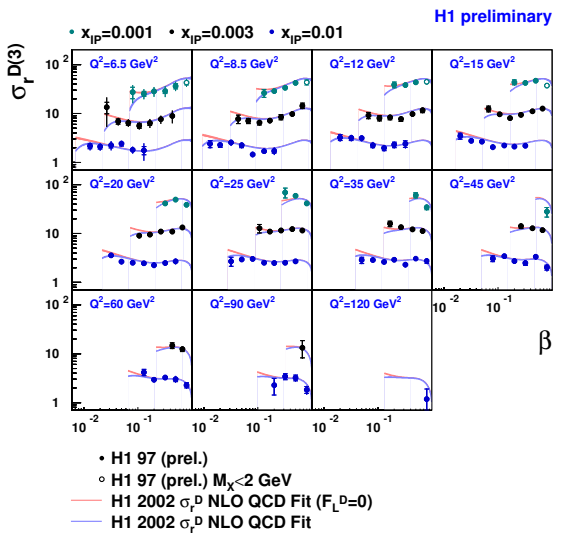

Figure 6. β dependence of the reduced cross section at fixed $x_{I\!P}$ and fixed Q^2 compared with the predictions of the NLO QCD fits.

production in DIS as a function of $z_{I\!P}^{jets}$, which represents the fraction of the hadronic energy in the final state contained in the two jets [15]. The measurement is compared with the predictions of the "resolved Pomeron" model, based on different sets of Pomeron gluon distributions obtained from the LO QCD fit as described above (labeled H1 2002 σ_r^D), and fits to earlier F_2^D data (labeled H1 Fit 3 and H1 Fit 2) [14]. Taking into account the considerable uncertainties in the parton densities, final state modeling uncertainties and higher order effects, there is an acceptable agreement with hard scattering factorization.

Figure 9 shows the diffractive D^* production cross section as a function of β [16]. The resolved Pomeron model, which uses the results of NLO QCD fits to diffractive DIS and γp data made by Alwero et al. (ACTW) [17], describes well both the shape and normalization of this cross section (as well as other cross sections which are not shown here). We note that in the ACTW fits Pomeron structure is also dominated by gluons.

The same D^* measurement is compared with the prediction of of a gluon exchange model due to Bartels et al. (BJLW) [18] and the "saturation model" of Golec-Biernat and Wüsthoff (SATRAP) [7]. Both models include significant $q\bar{q}g$ contributions to the partonic final state. The measurement is sensitive to the difference in these models: while SATRAP reproduces data distributions well, the BJLW model overestimates the data. On the other hand, the BJLW model, which contains only $q\bar{q}$ fluctuations, predicts too small cross section.

5. Diffractive Three Jet Production

Diffractive three jet events have been studied by the ZEUS experiment [19]. The differential jet shape $\rho(\phi)$, defined as the fraction of the jet energy which lies inside an annulus at angular distance ϕ around the jet axis, is shown in Figure 10 as a function of ϕ for the most forward and most backward jets. Here, the forward direction is defined to be the direction of the Pomeron. The jet in the Pomeron direction is broader then the jet

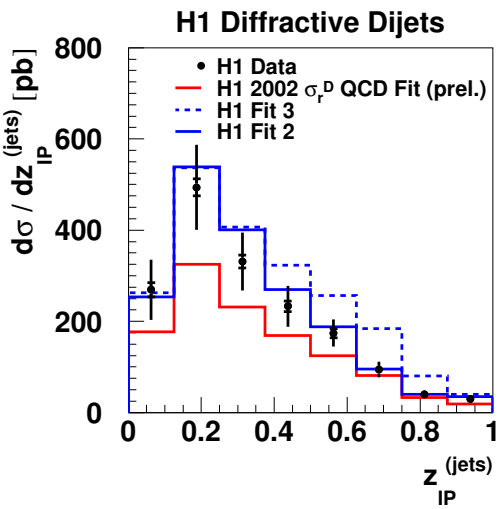

Figure 8. Diffractive dijet cross section differential in the fraction of the exchanged momentum transferred to the dijet system $z_{I\!P}^{jet}$ compared with the new and old LO QCD fits.

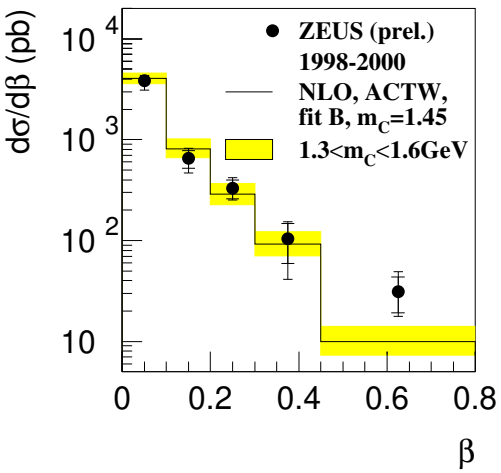

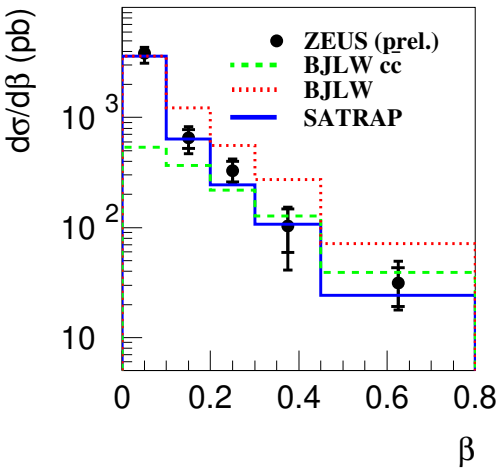

Figure 9. Differential cross section for $D^{*\pm}$ production in DIS as a function of the Pomeron momentum carried by struck quark, β.

in the photon direction. This result supports the picture in which three jet final state is dominated by $q\bar{q}g$ configurations with a gluon emitted in the Pomeron direction.

6. Conclusions

HERA is an ideal facility for the study of the transition from soft to hard diffraction, explored using different hard scales ($Q^2, M_q, p_T^{jet}, ...$).

The measurements of inclusive diffraction and the hadronic final state in diffractive DIS can be

described within a consistent picture. The results support QCD factorization with diffractive parton densities which are evolved according to the DGLAP equations and are dominated by the gluonic contribution.

A variety of diffractive DIS data are successfully described by several "resolved Pomeron" and "colour dipole" models.

Acknowledgements

I would like to thank the organizers for this interesting, stimulating and enjoyable conference.

REFERENCES

1. A. Donnachie and P. Landshoff, *Phys. Lett.* **B 296** (1992) 227.
2. For a review see M. McDermott, DESY 00-126 (2000).
3. H1 Collaboration, *Nucl. Phys.* **B 463** (1996) 3, Contributed paper 801 to EPS2001, Budapest.
4. ZEUS Collaboration, *Phys. Lett.* **B 377** (1996) 259, *Z. Phys.* **C 73** (1996) 73, *Eur. Phys. J.* **C 2** (1998) 247, *Phys. Lett.* **B 437** (1998) 432.
5. H1 Collaboration, *Phys. Lett.* **B 483** (2000) 23.
6. ZEUS Collaboration, *Eur. Phys. J.* **C 24** (2002) 345, *Phys. Lett.* **B 437** (1998) 432.
7. K. Golec-Biernat and M. Wüsthoff, *Phys. Rev.* **D 59** (1999) 014017, *Phys. Rev.* **D 60** (1999) 114023.
8. A.D. Martin, M.G. Ryskin and T. Teubner, *Phys. Rev.* **D 62** (2000) 14022; L. Frankfurt, M. McDermott and M. Strikman, *Journal High Energy Phys.* **103** (2001) 45.
9. ZEUS Collaboration, contributed paper 594 to EPS2001, Budapest.
10. H1 Collaboration, contributed paper 808 to EPS2001, Budapest.
11. J.C. Collins, *Phys. Rev.* **D 57** (1998) 3051, *Phys. Rev.* **D 61** (2000) 019902.
12. H1 Collaboration, contributed paper 980 to ICHEP2002, Amsterdam.
13. H. Jung, *Comp. Phys. Commun.* **86** (1995) 147.
14. H1 Collaboration, *Z. Phys.* **C 76** (1997) 613.
15. H1 Collaboration, *Eur. Phys. J.* **C 20** (2001) 29.
16. ZEUS Collaboration, DESY-02-082, submitted to Phys.Lett.B.
17. L. Alvero et al., *Phys. Rev.* **D 59** (1999) 074022.
18. J. Bartels, H. Lotter and M. Wüsthoff, *Phys. Lett.* **B 379** (1996) 239; J. Bartels et al., *Phys. Lett.* **B 386** (1996) 389.
19. ZEUS Collaboration, *Phys. Lett.* **B 516** (2001) 273.

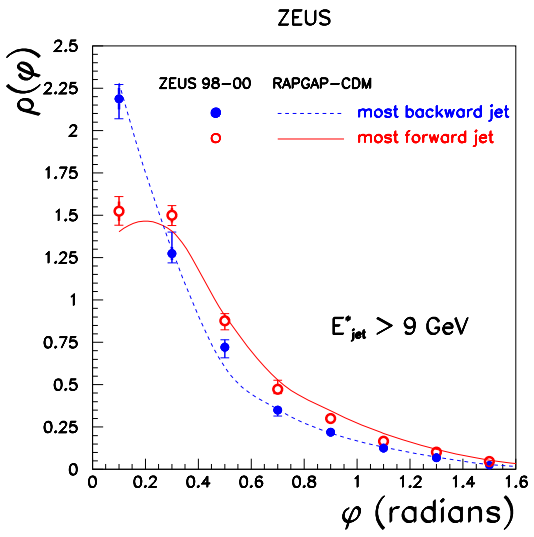

Figure 10. The differential jet shape $\rho(\phi)$ for the most forward and most backward jets in three–jet events. The forward direction is defined as the Pomeron direction.